

Halogen-free flame-retardant cable compounds: Influence of magnesium-di-hydroxide filler and coupling agent on EVA/LLDPE blend system morphology

Michael Heinz¹  | Christoph Callsen² | Waldemar Stöcklein¹ |
Volker Altstädt²  | Holger Ruckdäschel² 

¹Corning Optical Communications GmbH, Berlin, Germany

²Department Polymer Engineering, University of Bayreuth, Bayreuth, Germany

Correspondence

Volker Altstädt, Department Polymer Engineering, University of Bayreuth, Universitätsstraße 30, 95447 Bayreuth, Germany.

Email: volker.altstaedt@uni-bayreuth.de
Michael Heinz, Corning Optical Communications GmbH, Walther-Nernst-Str. 5, 12489 Berlin, Germany.
Email: michael.heinz@corning.com

Abstract

Objective of this work was to deeper understand the influence of a grafted coupling agent in EVA/LLDPE based blends containing mineral filler acting as a flame-retardant. EVA/LLDPE blends (50:50 phr) containing magnesium-di-hydroxide (MDH) were compounded. For comparison, parts (4%–5%) of LLDPE were substituted with MAA-g-LLDPE copolymer as a coupling agent. No influence of the coupling agent was observed by differential scanning calorimetry (DSC) thermal analysis. A strong influence of different filler ratios (0%–60%) was detected by rheological investigations. Morphological studies revealed significant differences in blend morphology and filler location caused by phase transition which is close to the 50:50 composition. The coupling agent improved the compatibility of the blend in that a reduced phase size could be observed. The addition of the coupling agent relocated the mineral filler from being mainly located in the EVA phase into the interphase and created a connection between both polymeric phases which resulted in improved thermo-mechanical performance.

KEYWORDS

coupling agent, EVA/LLDPE blend, flame retardant compound, halogen-free flame retardant, polymer blend

1 | INTRODUCTION

In the past, fiber optic data cables were mainly used in the network backbone, while the last portion close to the access points was covered by copper cables. Lately, the continuous increasing demand for more bandwidth drives fiber optic cables more into buildings. The most critical factor for cables in indoor application is the resistance against fire as this is directly related to people's safety. In 2011, the European Union released the construction product

regulation (CPR) which resulted in mandatory testing and CE marking of all products which are permanently installed in buildings beginning in June 2016. This new regulation came up with more stringent burn test procedures which increases the requirements for flame-retardant materials to be used in cable sheathing application.^[1]

Polymers are materials with a high variety in application space and performance and show easy processability at a relative low cost. This fits well to cable application and the high requirements in regard of mechanical

This is an open access article under the terms of the Creative Commons Attribution License, which permits use, distribution and reproduction in any medium, provided the original work is properly cited.

© 2021 The Authors. *Polymer Engineering & Science* published by Wiley Periodicals LLC on behalf of Society of Plastics Engineers.

performance and a continuous production process. Unfortunately, most polymers are highly flammable which results in increased fire risk. To overcome this disadvantage, it is possible to use flame-retardant additives which show different effects to protect the material during combustion. Flame retardants based on mineral fillers represent the largest portion of flame-retardant additives in the cable industry. This has a simple reason: a lower cost in comparison to organic solutions makes it economical attractive to be combined with commodities like polyolefins. Another advantage that should be mentioned is that the combustion gases are neither corrosive nor acidic, which enables them to be used indoors. The metal hydroxides work predominantly in the condensed phase, decompose endothermically and release water. This leads to a heat sink in the substrate and a dilution effect of the combustion gases.^[2] Aluminum trihydroxide (ATH) and magnesium dihydroxide (MDH) represent the major market share of these additives.^[3–6]

The trend in material development went toward the modification and combination of existing polymers to overcome their disadvantages and combine their strengths. Polymer blends can be categorized into miscible and immiscible systems as the majority.^[7] While miscible blends obey linear mixing rules or show positive deviation, the response in immiscible systems is more complex. The material performance is strongly related to the multiphase morphology and interphase effects. These are affected by the polymer properties, like rheological behavior, polarity, or elasticity ratio. Another important factor influencing the blend morphology is processing (shear rate, temperature profile, and cooling rate).^[8–11]

Typical immiscible polymers used in the wire and cable industry for halogen-free flame-retardant solutions are polyethylene and ethylene-vinyl-acetate (EVA).^[12] While polyethylene shows good thermal stability and mechanical strength, its flexibility and ability to take up high amount of mineral filler is limited. In this field, EVA shows very positive performance but comes with weaker thermo-mechanical properties.^[13] Immiscible LLDPE/EVA blends are widely used in applications like shrink-films and the cable industry.^[12] Even in a not compatibilized state, they are reported to show improved toughness, environmental stress cracking resistance, and filler uptake.^[4, 13] Nevertheless, signs of partial miscibility of the polymeric backbone in the melt state were reported.^[14–18] Faker et al.^[14] performed extensive investigations of rheological and mechanical properties of pure PE/EVA blends which were then correlated to the morphology.

The addition of rigid mineral flame-retardant fillers affects the material performance significantly in terms of higher modulus and improved burning behavior. In general, a homogenous dispersed and stable state leads to optimal properties, as every agglomerate is a defect and

reduces performance.^[19] The required quality of dispersive and distributive mixing must be provided by a proper compounding process.^[20, 21] The response of polymer blends to filler addition varies based on the polymer matrix type and the filler type. It is reported that increasing aspect ratio and matrix stiffness are beneficial for the elastic modulus.^[22] The compound stiffness increases with increasing amount of particulate fillers. This effect is used in many mechanical components but can be a disadvantage in the application as cable sheath due to reduced flexibility. In addition, a clear increase in melt viscosity with increasing filler content is reported. This results in processing difficulties and speed limitations in a continuous cable manufacturing process via extrusion.^[19, 20, 22–26]

From a threshold of 20 vol%, particle–particle interactions are reported to significantly increase because of the decreasing polymer ligament thickness.^[27] Therefore, organic coupling agents (CAs) are tailored to affect the particle–polymer interphase and to improve the mechanical performance.^[19, 28] The key performance is a strong connection between both materials which can be either achieved by chemical bonds, hydrogen bonds, Van der Waals forces, or miscibility effects.^[29] Typical CAs are organo-silanes or grafted co-polymers. The co-polymer backbone is often chosen from the matrix material or a miscible polymer to achieve coupling through entanglements. Both types of CAs are reported to improve the mechanical performance, processability, and flame retardancy.^[30–32]

In the past, the effects and efficiency of different co-polymeric CAs in filled polymers were investigated.^[19, 27–30] This was often quantified by the mechanical performance.^[28] Although the above mentioned material combinations found their application in the industry, the influence of grafted co-polymeric CAs on the morphology and properties of unfilled and filled immiscible EVA/LLDPE blend systems was not yet extensively studied. Therefore, in this work investigations were performed using a blend of EVA and linear-low-density polyethylene (LLDPE). A ratio of 50:50% was chosen to investigate the instable range in the phase morphology close to the expected phase inversion point. Subsequently, different amounts of MDH as flame retardant filler were added to investigate the system's response. In some samples, part of the LLDPE was substituted with maleic-acid-anhydride grafted LLDPE as a function of a CA.

2 | MATERIALS AND METHODS

2.1 | Materials

EVA with VA content of 24% and LLDPE were blended in a ratio of 1:1. Parts of the LLDPE (4%–5%) were

substituted with maleic-acid-anhydride grafted LLDPE (MAA-g-LLDPE) as a CA for the mineral filler. For more fundamental investigations on systems with a pure EVA polymer matrix, MAA-g-EVA with a VA content of 24% was also used as a CA. Properties of the polymeric raw materials are listed in Table 1, the values were taken from the supplier datasheets. The polymers were chosen as they represent typical grades used in wire and cable compounds and were used as received.

To improve the flame retardancy, Magnifin H-5 MDH from Huber was added. The chosen grade is uncoated with a specific surface (BET) of 4–6 m²/g. The particle size is given with d_{50} : 1.6–2.0 μm in the technical datasheet.

2.2 | Sample formulations

The prepared formulations are shown in Table 2. The amount of MAA-g-LLDPE CA was chosen based on supplier recommendations and then adjusted for the different filler amounts to achieve a ratio of 2 phr CA per 10 wt% of mineral filler. The unfilled sample with CA contains 5% of the MAA-g-LLDPE.

Prior to the investigations reported in this paper, the miscibility of the co-polymer in LLDPE was investigated in a range from 2.5% to 50%. The molecular structure of both polymers was compared by C13 NMR. In addition, mechanical, thermo-mechanical and rheological characterizations were performed. No signs of incompatibility were detected with the formulations in Table 2.

2.3 | Sample preparation

The ingredients were melting mixed at 150°C using a counter rotating laboratory mixer (Brabender 350E). After plasticization and blending of the two resins, the mineral filler was added stepwise to simulate a continuous compounding process. While increasing the screw rpm, the compound was mixed for additional 10 min to ensure a high quality of dispersion. All compounds were prepared using the same parameter setup in regard of temperature, time, and screw rpm. To identify signs of degradation, the melt temperature and mixer torque were continuously monitored. The compounds were removed from the mixer in a hot state and cut into smaller pieces. After cooling down at room temperature for at least 1 h, the pieces were grinded into pellet shape using a rotary mill.

In a second process, the pellets were then extruded into 1 × 20 mm wide strips using a 19 mm single screw extruder (L/D 25) with a 3-zone low compression screw (CR 1:2). The temperature profile was set to 150/160/170°C. Again, the melt temperature, pressure, and extrusion torque were monitored to identify potential signs of degradation or agglomerates of the flame-retardant filler.

2.4 | Characterization

2.4.1 | Differential scanning calorimetry (DSC)

The differential scanning calorimetry (DSC) was performed on a DSC Q2000 (TA Instruments) under nitrogen

TABLE 1 Data and properties of the polymeric ingredients

Type	EVA (24% VA)	LLDPE	MAA-g-EVA	MAA-g-LLDPE
Supplier	Arkema	Dow	Arkema	Silon
Grade name	Evatane 24-03	Dowlex 2045	Orevac 9304	Tabond 3044
comment	24% vinyl acetate content	Ziegler-Natta catalyzed grade	Modified EVA coupling agent	Modified LLDPE coupling agent
T_m	80°C	119°C	80°C	122°C
MFR (190 °C/2.16 kg)	3 g/10 min	1 g/10 min	7.5 g/10 min	1.6 g/10 min
Density	0.94 g/cm ³	0.92 g/cm ³	0.94 g/cm ³	0.94 g/cm ³

TABLE 2 Recipes of the prepared and tested formulations given in weight-%

	0% MDH	0% MDH + CA	30% MDH	30% MDH + CA	60% MDH	60% MDH + CA
EVA (24% VA)	50.0%	50.0%	35.0%	35.0%	20.0%	20.0%
LLDPE	50.0%	45.0%	35.0%	30.8%	20.0%	15.2%
MAA-g-LLDPE		5.0%		4.2%		4.8%
MDH			30.0%	30.0%	60.0%	60.0%

atmosphere. The samples were tested in aluminum pans with an empty pan as a reference. The temperature profile included a heat/cool/heat cycle from -60°C to 200°C in a heating/cooling rate of 10 K/min. To address the reduced polymer ratio in the samples containing mineral filler, weight correction was used. As the thermal capacity of the filler at such high loadings cannot be neglected, a baseline correction using a pure MDH curve was performed.

2.4.2 | Rheology

The rheological studies were performed using a parallel plate rheometer ARES-RDA III (TA Instruments) in strain control mode. The frequency sweeps were carried out from 100 to 0.1 rad/s at a temperature of 150°C and a shear deformation of 1%. Investigations of polymer stability were additionally carried out in a time sweep at 150°C , 1 rad/s and 10% deformation.

2.4.3 | Dynamic mechanical analysis

The thermomechanical properties were examined by means of dynamic mechanical analysis (Netzsch-Gabo Eplexor 500N). The samples were cut from extruded strips measuring 40×10 mm. This resulted in a free clamping length of 25 mm. The bars were measured under tension in the direction of extrusion. A temperature range from -100°C to $+100^{\circ}\text{C}$ was run through at a heating rate of 2 K/min. The applied frequency was 1 Hz. The tests were run under strain control with 0.5% static strain (maximum force 80 N) and 0.1% dynamic strain (maximum force 50 N).

2.4.4 | SEM microscopy

The morphology was investigated using electron microscopy in a SEM Zeiss Ultra Plus (voltage 3 kV). Cryo-fractured samples of the strips perpendicular to the extrusion direction were prepared using liquid nitrogen.

Parts of the samples were only stained, other parts only etched. Staining was performed with Ruthenium tetroxide vapor for 30 min. The etching procedure was chosen referring to Faker et al.^[14] and Wattananawinrat et al.^[33] to dissolve the EVA phase in xylene at 50°C for 6 h. Due to incomplete results in the small phase sizes in the filled samples, the method was adjusted. The extraction time was increased to 48 h and temperature to 60°C for all samples, while the solvent was constantly flowing. The samples were then platinum sputtered (1.5 nm), followed by a vaporized carbon layer (20 nm).

3 | RESULTS AND DISCUSSIONS

3.1 | Differential scanning calorimetry

The thermal analysis of the investigated systems is shown in Figure 1. The incompatible blends show separate melting peaks of EVA at 80°C and LLDPE around 120°C . The used LLDPE is a Ziegler-Natta catalyzed grade with randomly distributed comonomer content. This results in a broad melting curve below 120°C , followed by the polymer chains containing no co-monomer melting at 121°C . For the unfilled sample containing CA (0% MDH + CA), this characteristic shoulder around 121°C is replaced by a single peak. Deeper investigations of this effect have shown that this is related to a superposition by a more intensive and narrower melting peak of the MAA-g-LLDPE at 122°C . Differences in crystallinity could be ruled out by DSC and WAXS measurements.

Throughout the addition of flame-retardant filler (MDH), the peak positions and the effect of a peak shape change by the CA do not change. If CAs are used, an increase in the width of the melting peak at 110°C with increasing MDH content is observed. This is caused by the signal superposition of the steeper MAA-g-LLDPE melting peak with the LLDPE signal. The peak height increases with filler loading due to the increased CA ratio in the polymer fraction. An indicator of this is a reduced peak intensity at 121°C . The 60% MDH sample shows a slight difference in the area of this LLDPE melting peak. Therefore, the melting peaks of the samples without CA were compared and a difference of -0.6°C between the unfilled and the 60% MDH sample was calculated. Except for a slightly increased shoulder, no changes in peak position or crystallinity were observed.

3.2 | Rheology

To further understand the blend mixing dynamic and to calculate a phase inversion point, the pure blend components and the blends were characterized in parallel plate rheometry. It is expected that the viscosity of the blends is affected by the filler location: This can be the even distribution in both phases, only in one of each components or in the interface. To have a complete picture, pure EVA and LLDPE were compounded with 0%, 30%, and 60% filler ratio. To further understand the influence of the CA, the samples were additionally produced using 10% of the co-polymer (+CA). A comparative overview of the rheological analysis in frequency sweep is shown in Figure 2. The samples without CA are drawn in solid lines, the samples containing CA in dotted lines.

As expected, the viscosity levels of both polymers are increased by the addition of mineral filler. EVA does not show significant differences caused by the addition of the CA. All samples show shear thinning behavior. None of the samples show a clear Newtonian plateau at low frequency within the measurement range. The unfilled samples (0% MDH) show a plateau-like tendency which is reduced with increased filler amount. All samples containing 60% MDH show a steeper progression throughout the measurement range. Such increase in viscosity in combination with a reduced Newtonian-plateau for increased filler content in thermoplastic polymer was described by Poslinsky et al.^[25] An influence of the CA becomes visible at the highest filled LLDPE sample. While the 60% MDH shows a significant increase in viscosity at low frequency, this cannot be observed for the sample using CA. This “yield stress effect” was also reported by Laun^[34] after observing a viscosity increase to infinite

values toward lower shear rates of dispersed latex particles in emulsion. This observation is caused by filler particle-interlocking and is a sign of insufficient coupling or polymer coverage.

The tested EVA/LLDPE blends with different filler ratio and CA addition are shown in Figure 3. No significant influence of the CA can be observed for all amounts of filler loading. Both curves within the respective filler level are lying close to each other. Even for the 60% filled samples, no signs of increased filler–filler interaction, like the mentioned “yield stress effect” are observed.

The rheological measurements at the respective shear rate during compounding were used to determine the viscosity of the components in the compounder. The theoretical phase inversion of the incompatible blends can be calculated based on these and the following equation used by Faker et al.^[14] which was derived from Steinman et al.^[35]

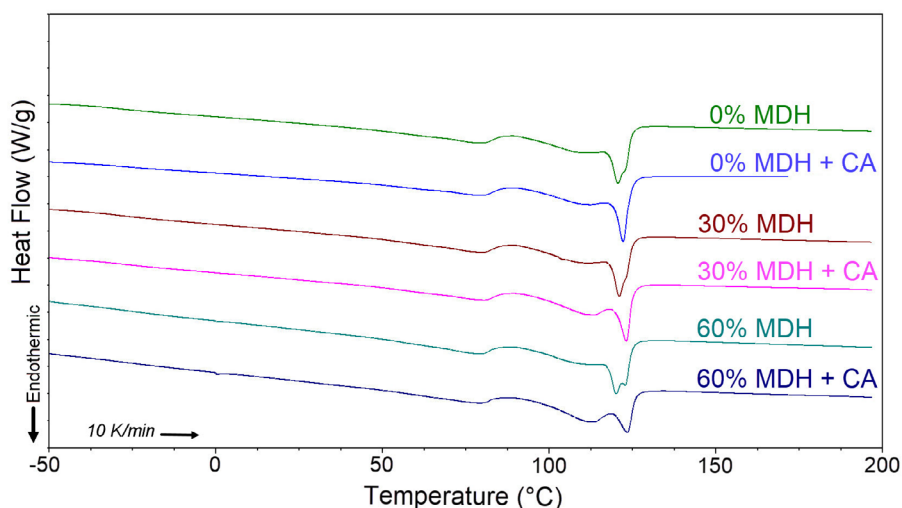


FIGURE 1 DSC measurements of the investigated compounds

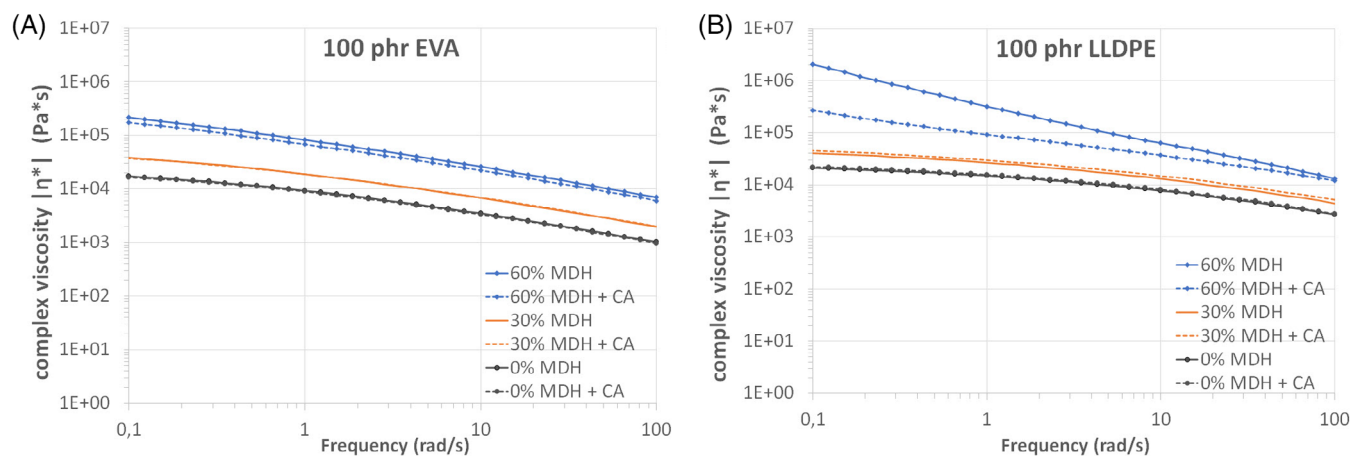


FIGURE 2 Parallel plate rheology of 0%, 30%, and 60% filled EVA (A) and LLDPE (B), with and without coupling agent (CA)

$$\phi_2 = -0.12 \log\left(\frac{\eta_1}{\eta_2}\right) + 0.48 \quad (1)$$

In the previously shown results, it can be observed, that the incorporation of filler affects the viscosity significantly. As it is not yet clear where the filler will be located, different scenarios needed to be considered in calculating the phase inversion points. In Table 3, the equation was applied to different combinations of rheological curves. This allowed to calculate the expected phase inversion points of the EVA/LLDPE morphology based on the filler location. The results for the unfilled samples (0% MDH) fit to the outcome reported by Faker et al.^[14] and Takidis et al.^[15] The phase inversion is mainly affected by the filler location. For the 60% filled sample, the CA in LLDPE causes additional influence which results from the observed differences in the viscosity curves. If the filler is located in both polymers, the phase inversion and so the expected phase size stays relatively stable. For the other two scenarios, the phase inversion ratio moves toward the polymer fraction that does not contain the filler.

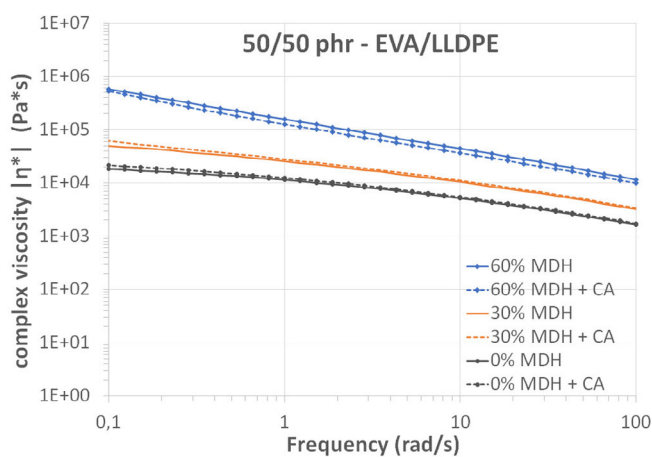


FIGURE 3 Parallel plate rheology of 0%, 30% and 60% filled 50/50—EVA/LLDPE blends with and without coupling agent (CA)

3.3 | Dynamic mechanical analysis

In order to examine and assess the mechanical performance of the materials over a wide temperature range, DMA tests were carried out. The samples made of pure EVA (a), pure LLDPE (b) and the 50/50 blend (c) filled with 0%, 30%, and 60% MDH with and without CA are shown in Figure 4. The storage modulus of all tested samples increases with increasing filler content. The EVA sample (a) shows a clear drop in the modulus around the glass transition temperature (-28°C), followed by a steep drop in the modulus near the melting temperature (80°C). It can be seen that a higher filler content slightly increases the heat resistance of the samples. When comparing the 0% and 60% samples, a shift in the thermomechanical parameters by 5°C – 10°C (modulus drop at Tg and Tm) can be observed. With all pure EVA samples (a), no influence from the added MAA-g-EVA as a CA is visible. Compared to EVA, pure LLDPE (b) shows better thermal stability with slow softening over the entire temperature range without noticeable drops. At temperatures below 0°C , no significant influence of the CA can be seen. At higher temperatures (e.g., over 50°C) the 60% filled samples with CA show an improvement in the modulus. The unfilled and the 30% sample show no significant difference caused by the adhesion promoter. Looking at the 50/50 mixtures (c), the modulus shows a decrease near the Tg of EVA (28°C). From this temperature on, the storage modulus curves of the samples with and without adhesion promoter begin to differ. The compounds with CA show improved thermomechanical properties, the greatest effect being observed in the 60% filled sample at higher temperatures. Even the melting range of EVA above 70°C is compensated. This is surprising because the CA used is based on LLDPE and an interaction with EVA was not to be expected.

The amount of improvement by adding the MAA-g-LLDPE CA to the 50/50 blend system was unexpected. It was not previously clear why the LLDPE-based CA is

TABLE 3 Calculated values of phase inversion ratio of EVA/LLDPE blends and compounds

Scenario	COUPLING	Calculated ratio of EVA/LLDPE phase inversion		
		0% MDH	30% MDH	60% MDH
Filler evenly distributed	–	47.9/52.1	48.6/51.4	48.5/51.5
	+CA	48.0/52.0	48.0/52.0	49.8/51.2
Filler only in EVA	–	47.9/52.1	51.4/48.6	58.4/41.6
	+CA	48.0/52.0	51.2/48.8	58.6/41.4
Filler only in LLDPE	–	47.9/52.1	45.1/54.9	38.0/62.0
	+CA	48.0/52.0	44.5/55.5	39.7/60.3

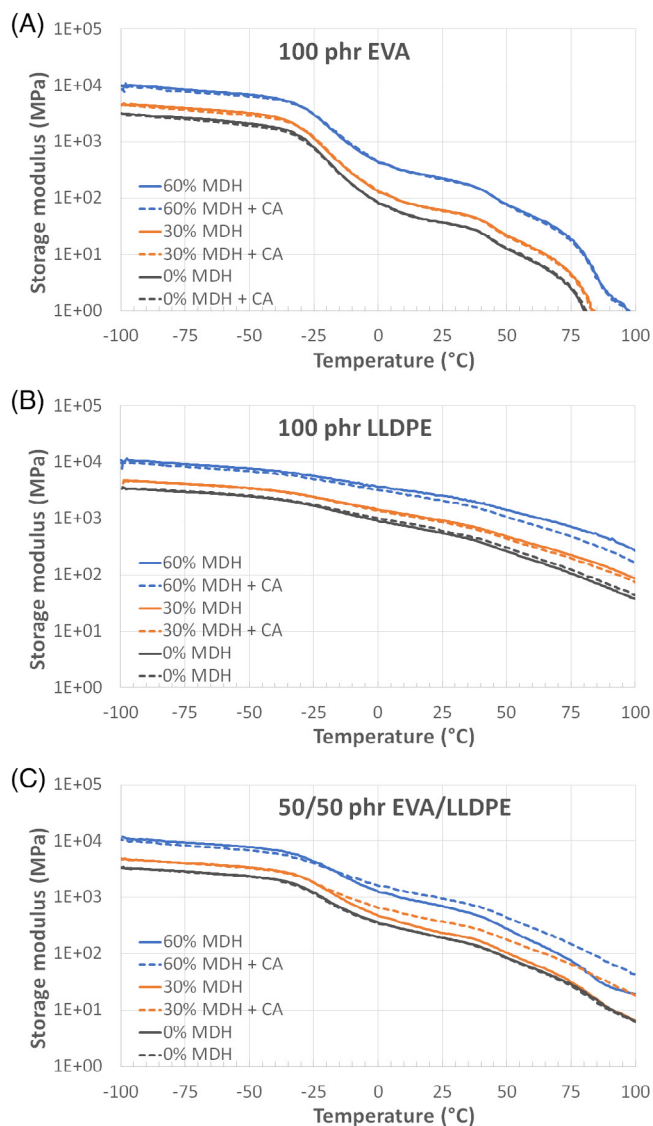


FIGURE 4 Dynamic mechanical analysis of 0%, 30% and 60% filled EVA (A), LLDPE (B), and 50/50 EVA/LLDPE (C) with and without coupling agent (CA)

able to improve the low heat resistance of the EVA in the 50/50 blend. The CA only made minor improvements in the case of pure LLDPE. The blends are therefore expected to have two separate polymer phases of EVA and LLDPE + MAA-g-LLDPE. Further studies on this effect are described in the following section.

3.4 | SEM analysis of cryo-fractured surfaces

The compound morphology was investigated using cryo-fractured surface analysis by SEM microscopy. To identify the polymer phases and to enhance the contrast, staining was used for sample preparation. The resulting

SEM images are shown in Figure 5. For a size comparison, the magnification was kept stable at 1000 \times . As the observed structures become smaller with increasing filler level, additional pictures with 10,000 \times are shown for both 60% MDH samples. The unfilled polymer blends can be identified due to the enhanced contrast. It is visible, that the phase sizes of the sample with and without CA differ. It is not yet clear which of the two polymers is reduced in phase size. Based on the ductile cryo-fracture behavior at the phase limits, it is likely the LLDPE. It is also not clear if the phase size is reduced or the morphology changes from co-continuous to droplet. This effect will be deeper investigated in the following section.

The polymeric phases of the blends can still be recognized in the 30% MDH sample. In addition, it is observable that the filler is mainly located in one phase. Looking at the 30% MDH + CA sample, the blend morphology can be hardly identified. The filler seems to be more evenly distributed throughout the sample. Due to the increasing amount of filler, the blend morphology is not visible in the 60% filled samples, not with nor without CA. In general, the sample with CA shows a finer structured fracture surface. This is a sign for improved coupling and reduced polymer phase sizes. This can be seen at the images taken with higher magnification. The filler particles are surrounded by a finer structured morphology. Contrary to the expectations, signs of polymer-filler interaction can also be observed for the sample without CA.

Further investigations to determine the filler location were tried using TEM microscopy, but the filler caused sample break during microtome cutting. A try to cut the samples with an ion-beam degraded the polymers. TEM microscopy of thicker samples was still performed but the contrast between both polymers was lost due to the high intensity of the filler. Therefore, to further investigate the morphology and filler location, cryo-fractured samples were etched to remove the EVA phase.

3.5 | SEM analysis of the etched samples

To investigate the morphology more in detail, cryo-fractured samples were etched to remove the EVA portion. The residual structures can be seen in Figure 6 with a magnification of 1000 \times to judge the morphology. Deeper investigations about the filler location using a higher magnification are following in the next section.

Comparing the unfilled samples, it is visible that the addition of a CA reduces the phase size of the LLDPE while maintaining a co-continuous morphology. This is a sign for increased compatibility of the immiscible blend. It is assumed that this effect is caused by an increase in

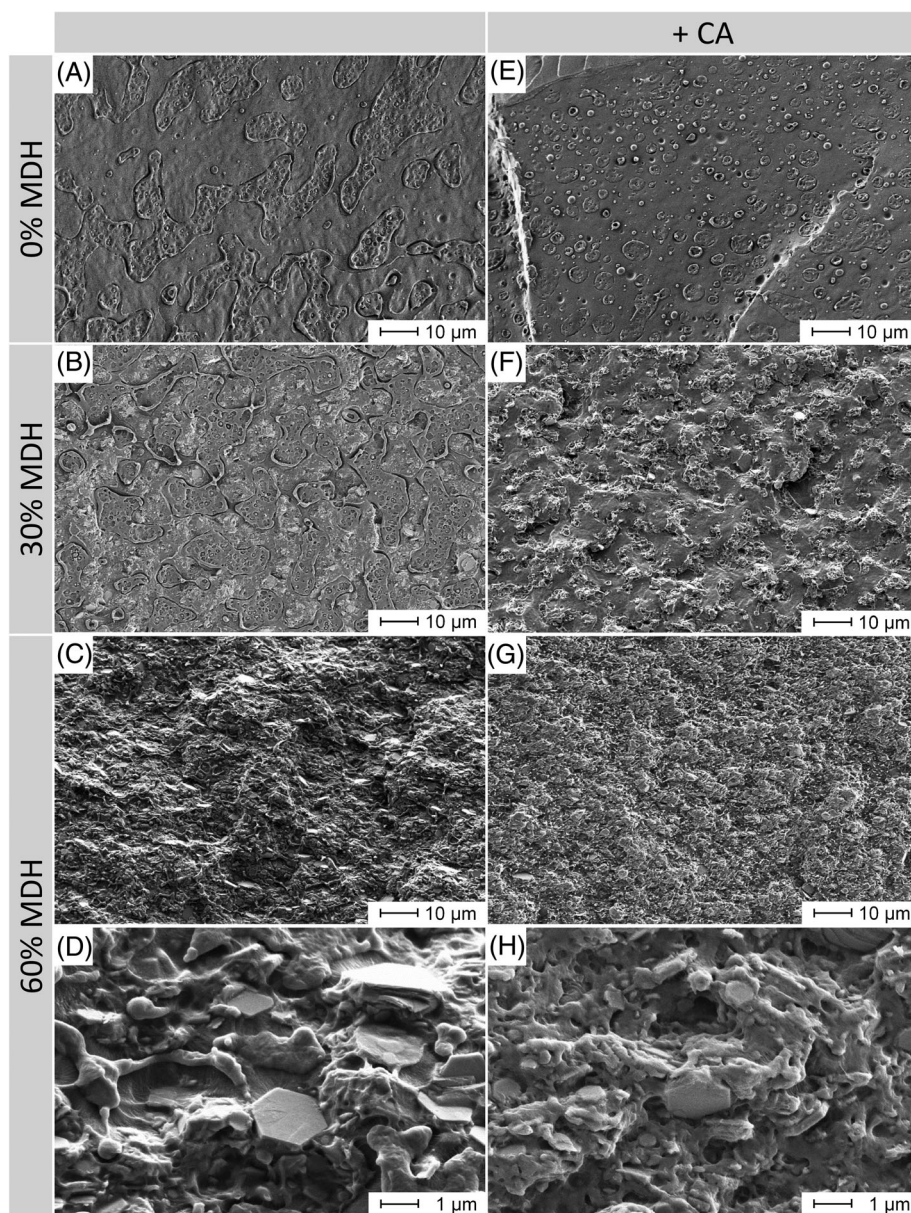


FIGURE 5 SEM images of cryo-fractured and RuO₄ stained surfaces of pure 50/50 EVA/LLDPE blends (A), filled with 30% MDH (B), 60% MDH (C, D) without coupling agents and the same filler dosage with coupling agent (E–H)

polarity of the LLDPE + CA fraction as no significant change in melt viscosity and DSC was observed. The addition of 30% filler decreases the LLDPE phase size of both sample variants, the effect of the CA resulting in further reduced LLDPE phase size is maintained. Comparing the LLDPE residue, the sample without CA shows a smooth surface of the interface and no inclusions of flame-retardant filler in the LLDPE. In comparison to this, the residue of the sample with CA shows very rough structures which seem to consist of flame retardant. The morphology is getting even finer when looking at the 60% filled samples. The effect of smaller phases due to the CA can be clearly seen for all samples, with and without filler, which supports the theory of increased polarity. Co-continuity of the LLDPE fraction is maintained throughout all samples.

3.6 | Determination of filler location

For easier determination of the filler location, the etched samples were investigated with higher magnification, see Figure 7. Significant differences in between the samples with and without CA can be observed. Looking at the samples without CA, the filler was completely removed with the EVA phase. Only a few stray particles remained on the sample surface after etching. A check for inclusions was performed by optical investigation of the cryo-fracture plane and EDX analysis—no filler was detectable in the LLDPE phase.

Analyzing the samples containing CA, it can be observed that the flame-retardant filler remains after etching. The filler is located at the LLDPE surface which represents the blend interface between LLDPE

FIGURE 6 SEM images of cryo-fractured and xylene etched surfaces of pure 50/50 EVA/LLDPE blends (A), filled with 30% MDH (B), 60% MDH (C) without coupling agents and the same filler dosage with coupling agent (D–F)—magnification 1000 \times

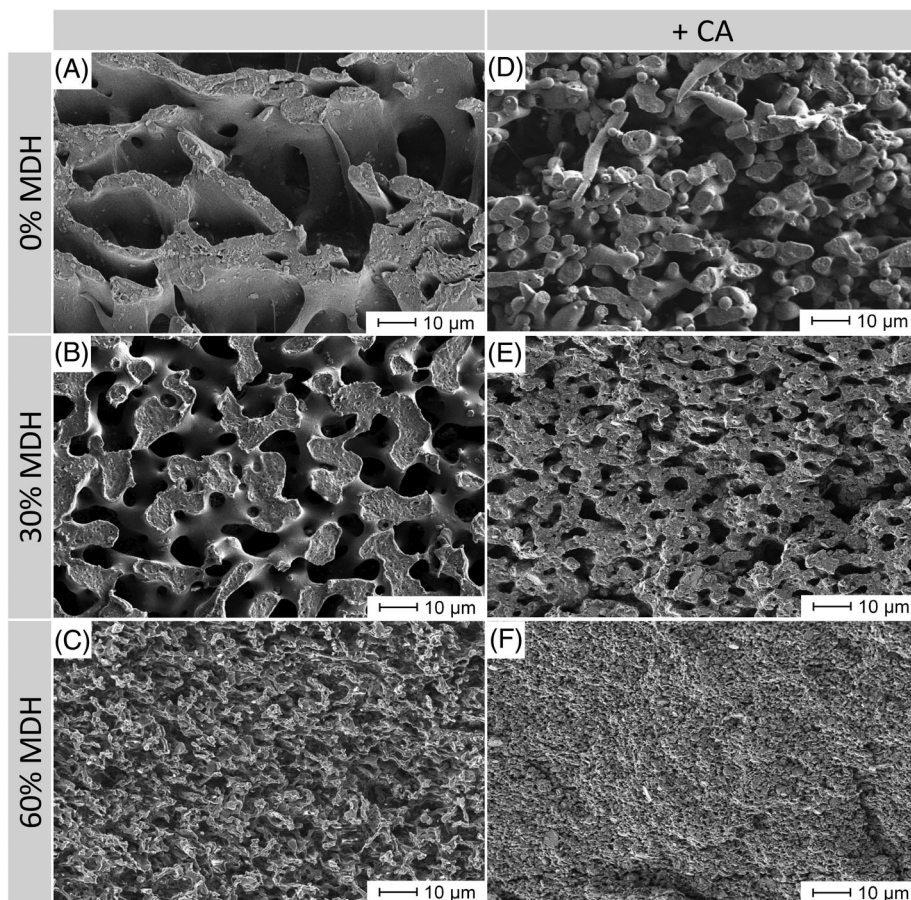
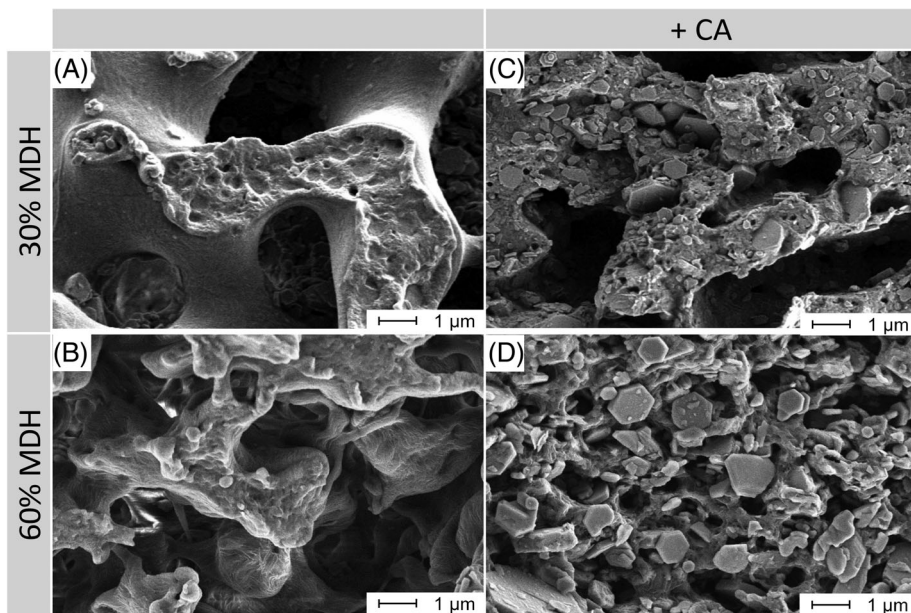


FIGURE 7 SEM images of cryo-fractured and xylene etched surfaces of 50/50 EVA/LLDPE blends filled with 30% MDH (A), 60% MDH (B) without coupling agents and the same filler dosage with coupling agent (C, D)—magnification 10,000 \times



and EVA. In some cases, filler was partially stuck in the LLDPE but a check for filler inclusions in the LLDPE using EDX on the larger fracture surfaces was negative. All particles seen at the surface show free space where the EVA was located. It can also be seen

that the polymeric phases become smaller with increased filler content (60% MDH) resulting in a phase diameter close to the filler particle size. Here, a determination of the filler location was not possible anymore.

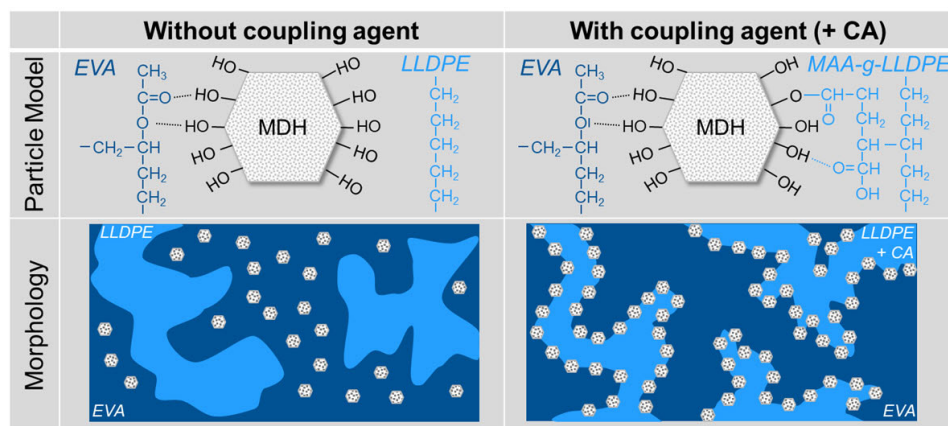


FIGURE 8 Graphical model of the polymer–filler interactions with and without coupling agent

4 | CONCLUSIONS

The investigations of the systems with different degrees of filling have shown that neither the use of adhesion promoters nor the filler content change the crystallinity of the investigated EVA/LLDPE-based compounds. Nevertheless, an influence of nucleation on the crystallization cannot be completely ruled out.

The viscosity curve of the EVA/LLDPE blends showed a clear influence of the filler content, but no influence of the CA. Pure LLDPE samples with a high filler content (60%) showed particle–particle interactions that could be reduced by using a CA. This effect does not occur when EVA is present in the blend. This is to be regarded as an indicator for an interaction between MDH and EVA, but not for an interaction with LLDPE. The inversion points of the mixed phase are influenced by the filler distribution between the two polymer phases. It was possible to theoretically calculate the phase inversion points of each scenario based on the viscosity measurements for specific compound components and mixtures. These results were later confirmed by morphological studies.

The use of mineral fillers and CAs has led to considerable improvements in the thermomechanical behavior of the compounds. This was most pronounced at elevated temperatures. The use of adhesion promoters, especially in the 50/50 EVA/LLDPE blends, led to a significant improvement in the thermomechanical properties. The earlier softening of the EVA phase is compensated by the more stable LLDPE phase in the presence of MAA-g-LLDPE and filler, although both polymer phases remain immiscible.

Morphological investigations proved the immiscibility of the blend system. The LLDPE structures are dispersed more finely by adding the CA. This is a sign of an increase in compatibility and could be caused by an increase in the polarity of the LLDPE phase due to functional maleic acid anhydride groups in the CA. The small amount of CA in the system is the reason that its influence is small and obviously cannot overcome

immiscibility in the blend system. It must be taken into account that this leads to an increase in the size of the interface in the mixed phase and possibly supports the observed effect of filler displacement into the interface.

In the filled samples, the LLDPE phase becomes finer with increasing filler content. This is caused by the flame-retardant filler as the third component in the blend. In addition, specific imperfections were identified. In samples without an adhesion promoter, no filler was found in the LLDPE phase. This observation is made in a publication by Tham et al.^[36] confirmed in 2016, which describes the interactions of EVA and the OH groups of uncoated silicon dioxide through hydrogen bonds. Since the EVA + filler content increases with increasing content, the LLDPE phase shrinks. The observed morphology fits well with the previously calculated results from the rheological measurements and also confirms a clear shift of the phase inversion point to the LLDPE.

Upon closer examination of the samples containing the CA, it was observed that flame-retardant filler can also be found in the LLDPE phase. Based on further investigations, it was found that the flame retardant is located in the intermediate phase between LLDPE and EVA.

This leads to the theory that the filler, in combination with the adhesion promoter, creates a bond between the components of the polymer mixture. For further clarification, a graphic model is shown in Figure 8. EVA interacts with the flame-retardant filler via hydrogen bonds. In systems without an adhesion promoter, the LLDPE has no chance of interacting with the filler. By adding the CA based on LLDPE, the LLDPE phase interacts with the filler chemically through covalent and physically through hydrogen bonds. This presumably causes the filler to reach the interface, which creates a strong interaction with the polymers and thus a finer morphology.

ACKNOWLEDGMENT

The authors are thankful for the support from the Bavarian Polymer Institute (BPI) for using the SEM

capabilities and the companies Huber, Silon, DOW and Arkema for providing the sample materials and further technical information. Finally, the authors are deeply thankful to Mr. Alexander Kiel for compounding and testing, Mrs. Ute Kuhn for thermal and rheological analysis and Mrs. Annika Pfaffenberger for the scanning electron micrographs. Open Access funding enabled and organized by Projekt DEAL.

ORCID

Michael Heinz  <https://orcid.org/0000-0002-0237-4140>

Volker Altstädt  <https://orcid.org/0000-0003-0312-6226>

Holger Ruckdäschel  <https://orcid.org/0000-0001-5985-2628>

REFERENCES

- [1] ZVEI e.V., White Paper: Brandschutzkabel erhöhen die Sicherheit. <https://www.zvei.org/presse-medien/publikationen/white-paper-brandschutzkabel-erhoehen-die-sicherheit/>, 2017.
- [2] G. Skinner, Flame retardancy: the approaches available. in *Polymer Additives*, Springer Science, Boston, MA 1998, p. 260.
- [3] Y. Z. Wang, Halogen free flame retardants. in *Advances in fire retardant materials*, Woodhead Publishing, Cambridge, England 2008, p. 67.
- [4] S. C. Brown, Flame retardants: inorganic oxide and hydroxide systems. in *Plastics Additives*, Springer Science, Boston, MA 1998, p. 287.
- [5] R. Sauerwein, Mineral Filler Flame Retardants. in *Non-Halogenated Flame Retardant Handbook*, Scrivener Publishing LLC, Beverly, MA 2014, p. 75.
- [6] S. Kim, *Polym. Phys.* **2003**, 41(9), 936. <https://doi.org/10.1002/polb.10453>
- [7] L. A. Ultracki, *Polymer alloys and blends: Thermodynamics and rheology*, Hanser, Liberty Twp, Ohio 1989.
- [8] M. J. Folkes, P. S. Hope, *Polymer blends and alloys*, Chapman and Hall, London, England 1993.
- [9] O. Olabisi, L. M. Robertson, M. T. Shaw, *Polymer-polymer miscibility*, Academic Press, Cambridge, Massachusetts 1979, p. 1. <https://doi.org/10.1016/B978-0-12-525050-4.X5001-X>
- [10] D. R. Paul, C. B. Bucknall, Polymer blends. in *Performance*, Vol. 2, John Wiley and Sons, Hoboken, New Jersey 1999.
- [11] L. Ultracki, *Commercial Polymer blends*, Chapman and Hall, London, England 1998, p. 83.
- [12] K. Cousins, Polymers for Wire and Cable. in *Changes Within an Industry*, iSmithers Rapra Publishing, Shrewsbury, England 2000.
- [13] B. Borsova, J. Kressler, *Macromol. Mater. Eng.* **2003**, 288(6), 509. <https://doi.org/10.1002/mame.200390048>
- [14] M. Faker, M. K. Razavi Anghjeh, M. Ghaffari, S. A. Seyyedi, *Polym. J.* **2008**, 44(6), 1834. <https://doi.org/10.1016/j.eurpolymj.2008.04.002>
- [15] G. Takidis, D. N. Bikiaris, G. Z. Papageorgiou, D. S. Achillas, I. Sideridou, *J. Appl. Polym. Sci.* **2003**, 90(3), 841. <https://doi.org/10.1002/app.12663>
- [16] H. A. Khonakdar, U. Wagenknecht, S. H. Jaferi, R. Hassler, H. Eslami, *J. Adv. Polym. Technol* **2004**, 23(4), 307. <https://doi.org/10.1002/adv.20019>
- [17] H. A. Khonakdar, S. H. Jaferi, A. Yavari, A. Asadinezhad, U. Wagenknecht, *Polym. Bull.* **2005**, 54, 75. <https://doi.org/10.1007/s00289-005-0365-6>
- [18] I. Ray, D. Khashtgir, *Polymer* **1993**, 34(19), 2030. [https://doi.org/10.1016/0032-3861\(93\)90727-R](https://doi.org/10.1016/0032-3861(93)90727-R)
- [19] C. Dearmitt, R. Rother, Surface Modifiers for Use with Particulate Fillers. in *Fillers for Polymer Applications*, Springer, New York City 2017, p. 30.
- [20] J. Móczó, B. Pukánszky, Particulate Fillers in Thermoplastics. in *Fillers for Polymer Applications*, Springer, New York City 2017, p. 53.
- [21] D. M. Kalyon, A. Lawal, R. Yaziki, P. Yaras, S. Railkar, *Polym. Eng. Sci.* **1999**, 39, 6. <https://doi.org/10.1002/pen.11501>
- [22] M. M. Rueda, M. Auscher, R. Fulchiron, T. Périé, G. Martin, P. Sonntag, P. Cassagnau, *Prog. Polym. Sci.* **2017**, 66, 22. <https://doi.org/10.1016/j.progpolymsci.2016.12.007>
- [23] D. Bonn, M. M. Denn, L. Berthier, T. Divoux, S. Manneville, *Rev. Mod. Phys.* **2017**, 89(3), 2. <https://doi.org/10.1103/RevModPhys.89.035005>
- [24] M. Pishvaei, C. Graillat, P. Cassagnau, *Polymer* **2005**, 46(4), 1235. <https://doi.org/10.1016/j.polymer.2004.11.047>
- [25] A. J. Poslinski, M. E. Ryan, R. K. Gupta, S. G. Seshadri, F. J. Frechette, *J. Rheol.* **1988**, 32, 703. <https://doi.org/10.1122/1.549987>
- [26] D. M. Bigg, *Polym. Eng. Sci.* **1983**, 23(4), 206. <https://doi.org/10.1002/pen.760230408>
- [27] C. Kumudinie, Polymer-Ceramic Nanocomposites: Interfacial Bonding Agents. in *Encyclopedia of Materials: Science and Technology*, Pergamon, Oxford, England 2001, p. 7574.
- [28] J. Z. Liang, R. K. Y. Li, *Polym. Int.* **2000**, 49(2), 170. [https://doi.org/10.1002/\(SICI\)1097-0126\(200002\)49:2<170::AID-PI322>3.0.CO;2-U](https://doi.org/10.1002/(SICI)1097-0126(200002)49:2<170::AID-PI322>3.0.CO;2-U)
- [29] J. D. Miller, H. Ishida, Adhesive-Adherend Interface and Interphase. in *Fundamentals of Adhesion*, Springer, Boston, MA 1991, p. 291.
- [30] E. P. Pueddemann, Adhesion through silane coupling agents. in *Fundamentals of Adhesion*, Springer, Boston, MA 1991, p. 279.
- [31] A. I. Moncada, W. Huang, N. Horstman, Polyethylene Modification by Reactive Extrusion. in *Handbook of Industrial Polyethylene and Technology*, Scrivener Publishing, Beverly, MA 2017, p. 715.
- [32] C. A. Correa, C. Razzino, E. Hage, *J. Thermopl. Comps. Mater.* **2007**, 20(3), 323. <https://doi.org/10.1177/0892705707078896>
- [33] K. Wattananawinrat, P. Threepopnatkul, C. Kulsethanchalee, *Energy Procedia* **2014**, 56, 1. <https://doi.org/10.1016/j.egypro.2014.07.125>
- [34] H. M. Laun, *Angew. Makromol. Chem.* **1984**, 123, 335. <https://doi.org/10.1002/apmc.1984.051230115>
- [35] S. Steinmann, W. Gronski, C. Friedrich, *Polymer* **2001**, 42(15), 6619. [https://doi.org/10.1016/S0032-3861\(01\)00100-8](https://doi.org/10.1016/S0032-3861(01)00100-8)
- [36] D. Q. Tham, N. T. T. Trang, N. T. Chinh, G. V. Nguyen, *Green Proc. Synth.* **2016**, 5, 6. <https://doi.org/10.1515/gps-2016-0044>

How to cite this article: M. Heinz, C. Callsen, W. Stöcklein, V. Altstädt, H. Ruckdäschel, *Polym. Eng. Sci.* **2022**, 62(2), 461. <https://doi.org/10.1002/pen.25858>